Università della Svizzera italiana (USI)
Master in Computational Science
WS 2025/26

Modelling the Dynamics of a Temperature-Stressed Marine Predator–Prey System

Submitted by:
Vishal Rakhecha
Lugano, Ticino, Switzerland

Field of Study: Computational Science

Submitted to:
Professor Francisco Javier Richter Mendoza
Course: Introduction to Ordinary Differential Equations

Submission Date: January 15, 2026

Abstract

This report develops and analyzes a temperature-dependent Rosenzweig–MacArthur predator–prey model to investigate how ocean warming affects the stability and persistence of marine ecosystems. Using dynamical systems theory and numerical simulation, I identify a critical temperature threshold $T_c \approx 13.86$°C beyond which stable coexistence becomes impossible due to elevated predator mortality rates. The analysis employs linearization via the Jacobian matrix, the trace–determinant stability criterion, and high-resolution bifurcation diagrams (200 temperature points) to validate analytical predictions. Numerical results confirm theory to within 0.2% precision. The model demonstrates that relatively modest temperature increases (3–4°C) can trigger predator extinction through a transcritical bifurcation. The findings suggest that marine ecosystems face critical thermal thresholds under ongoing climate change, with implications for fisheries management and conservation strategy.

Keywords: predator–prey dynamics, temperature dependence, bifurcation analysis, dynamical systems, climate change, marine ecosystems, Rosenzweig–MacArthur model

Contents

1 Introduction

1.1 Motivation and Context

Predator-prey systems are fundamental models in mathematical ecology, capturing the essence of trophic interactions that structure biological communities. The classical Lotka-Volterra model, introduced in the 1920s, demonstrated that simple nonlinear ODEs could generate oscillatory population dynamics without external forcing. This work established a paradigm: dynamical systems theory provides powerful tools for understanding population regulation in ecological networks.

However, classical predator-prey models treat system parameters (growth rates, mortality rates) as constants. In reality, environmental variation, particularly temperature, exerts profound effects on metabolic rates and population dynamics. Warmer ocean temperatures increase metabolic rates in ectothermic organisms, accelerating both predator mortality and prey growth. This temperature-dependence can fundamentally destabilize coexistence equilibria, creating a mechanism for warming-induced ecosystem collapse.

1.2 Scientific Question

This project addresses a specific question: "At what temperature does stable predator-prey coexistence become impossible?" We model this by incorporating temperature-dependent metabolic rates into the Rosenzweig-MacArthur predator-prey system, a well-established framework in theoretical ecology. The key asymmetry in our model is that predators are more temperature-sensitive than prey, a pattern observed across marine ecosystems where ectothermic predators face higher metabolic costs from warming.

1.3 Approach

We employ three complementary analytical and numerical techniques:

1. **Analytical framework:** We derive equilibrium conditions and construct a bifurcation criterion that predicts the critical temperature threshold. Stability is assessed via the Jacobian matrix and linear stability analysis.

2. **Numerical bifurcation analysis:** We compute equilibrium populations and their stability across a range of temperatures (10–25°C), identifying the precise transition point separating coexistence from predator extinction.

3. **Time-series simulation:** We integrate the full nonlinear ODE system across four representative temperature scenarios to visualize population dynamics and validate the analytical predictions.

1.4 Project Objectives

The specific objectives are:

1. Formulate a temperature-dependent Rosenzweig-MacArthur ODE system with explicit temperature scaling laws for metabolic rates.
2. Analytically determine all equilibrium points and classify their stability as functions of temperature.
3. Identify the critical temperature T_c at which a transcritical bifurcation occurs, separating stable coexistence from predator extinction.
4. Numerically compute bifurcation diagrams and validate analytical predictions through high-resolution simulations.
5. Interpret results in the context of marine ecosystem stability and the potential for temperature-driven tipping points.

1.5 Code and Data Availability

The complete source code, numerical data, and figures are available on GitHub at:

https://github.com/vishalrakhecha18102000-debug/predator-prey-temperature-ode

All simulations are fully reproducible using Python 3.8+ with NumPy, SciPy, and Matplotlib. The repository includes parameter configuration files, data files in CSV format, and high-resolution PNG figures.

2 Mathematical Model

2.1 Problem Description and Model Motivation

I study a marine ecosystem consisting of a single prey species (small fish or zooplankton) and a single predator species (larger fish). Understanding predator–prey dynamics in changing thermal environments is increasingly urgent: ocean temperatures are rising due to climate change, threatening marine biodiversity and fisheries productivity worldwide. In the absence of environmental forcing, such systems naturally exhibit oscillatory dynamics. However, both prey growth rates and predator mortality rates depend on temperature. This temperature dependence is governed by fundamental metabolic scaling laws: biological rates increase with temperature over physiologically relevant ranges. Our goal is to understand how increasing ocean temperature affects the stability of the predator–prey equilibrium and the long-term persistence of both species.

2.2 State Variables and Parameters

I model the densities of prey and predator populations as continuous quantities. Let

$$R(t) \geq 0 \quad \text{denote the prey density (individuals per m}^3\text{) at time } t \text{ (days),} \tag{1}$$

$$P(t) \geq 0 \quad \text{denote the predator density (individuals per m}^3\text{) at time } t \text{ (days).} \tag{2}$$

The model is governed by the following parameters:

- $r(T)$: intrinsic growth rate of the prey population, which depends on temperature T;
- $K > 0$: carrying capacity of the prey population;
- $a(T)$: predator attack rate (encounter rate), which depends on temperature T;
- $b > 0$: predator conversion efficiency (fraction of consumed prey biomass converted to predator reproduction);
- $d(T)$: per-capita mortality rate of the predator population, which depends on temperature T;
- T: ambient sea temperature (in $^\circ$C), treated as a slowly varying or fixed control parameter on the timescale of population dynamics.

Specific numerical values for these parameters will be introduced in Section 2.5, where they are contextualized within the numerical experiments.

2.3 Modelling Assumptions

Our model rests on the following explicit assumptions:

1. **Well-mixed populations:** Prey and predator are uniformly distributed in the habitat (no spatial structure or migration). This is reasonable for a local water column or defined region.
2. **Continuous time and deterministic dynamics:** I ignore stochastic fluctuations (environmental noise, demographic chance) and treat populations as continuous variables. This is valid when populations are large ($R, P \gg 1$).
3. **Logistic prey growth:** In the absence of predators, prey grows logistically with carrying capacity K. This accounts for intraspecific competition or resource limitation.
4. **Linear predation rate (Holling Type I):** The rate at which predators encounter prey is proportional to prey density. This is a simplification; saturation effects (Holling Type II) occur at very high prey densities but are negligible in our parameter regime.
5. **Temperature as a quasi-static parameter:** I treat temperature T as a slowly varying (or constant on short timescales) control parameter. This is appropriate for seasonal or long-term climate change studies.
6. **Exponential temperature dependence:** Metabolic rates scale with temperature using exponential functions, a standard assumption in ecological population models.
7. **No age structure or life stage heterogeneity:** All individuals are identical in age and reproductive capacity, which simplifies the model but sacrifices some realism.
8. **Constant conversion efficiency:** The fraction b of consumed prey that converts to predator biomass is temperature-independent.

2.4 Temperature-Dependent Rates

Biological rates in marine ectotherms increase with temperature. Following standard modeling practice in population dynamics,I represent this dependence using exponential functions. Specifically:

$$r(T) = r_0 \exp(\alpha_r T), \quad r_0 > 0,\ \alpha_r \geq 0, \tag{3}$$

$$d(T) = d_0 \exp(\alpha_d T), \quad d_0 > 0,\ \alpha_d \geq 0, \tag{4}$$

$$a(T) = a_0, \quad a_0 > 0 \quad \text{(constant)}, \tag{5}$$

where r_0, d_0, a_0 are baseline rates at a reference temperature, and α_r, α_d are temperature sensitivity coefficients.

This exponential form is widely used in ecological ODEs because it captures the typical 3–5% per $^\circ\mathrm{C}$ metabolic rate increase observed in marine ectotherms over physiologically relevant temperature ranges. The choice to keep $a(T)$ constant is a simplification; in reality, encounter rates may also be temperature-dependent. However, this choice focuses the analysis on the competing effects of enhanced prey growth and increased predator mortality under thermal stress.

2.5 Numerical Parameter Values

For the numerical experiments presented in Section 4, I employ the following baseline parameter values, chosen to be biologically plausible for a marine predator–prey system:

- $\mathbf{r_0 = 0.5\ day^{-1}}$: baseline prey intrinsic growth rate. This value implies a prey population doubling time of $\ln(2)/r_0 \approx 1.4$ days under optimal conditions, consistent with rapid reproduction rates of zooplankton and small fish larvae.

- $\mathbf{K = 100\ individuals/m^3}$: prey carrying capacity. This represents a moderate population density typical of coastal oligotrophic waters, where nutrient limitation prevents extremely high densities.

- $\mathbf{a_0 = 0.01\ (predator \cdot day)^{-1}}$: predator attack rate (Holling Type I functional response coefficient). This parameter controls the encounter rate between predators and prey, scaled per predator individual and per day.

- $\mathbf{b = 0.2}$: predator conversion efficiency (dimensionless). This means that 20% of consumed prey biomass is converted into predator biomass and reproduction, with the remaining 80% allocated to respiration, activity, and maintenance. This value falls within the typical range of 10–25% observed for aquatic ectothermic predators.

- $\mathbf{d_0 = 0.1\ day^{-1}}$: baseline predator per-capita mortality rate at reference temperature. A constant death rate at baseline temperature implies an average lifespan of $1/d_0 = 10$ days for the predator population, reasonable for small fish or planktonic larvae.

- $\alpha_{\mathbf{r}} = \mathbf{0.02}\ ^\circ\mathbf{C}^{-\mathbf{1}}$: temperature sensitivity coefficient for prey growth rate. This coefficient implies that prey growth increases by approximately $\exp(0.02 \times 1) - 1 \approx 2\%$ per degree Celsius increase in temperature, representing modest metabolic acceleration.

- $\alpha_{\mathbf{d}} = \mathbf{0.05}\ ^\circ\mathbf{C}^{-\mathbf{1}}$: temperature sensitivity coefficient for predator mortality rate. This is 2.5 times larger than α_r, reflecting the empirical observation that ectothermic predators are often more temperature-sensitive than their prey. A 5% per °C increase in mortality with warming reflects elevated metabolic costs and reduced survival under thermal stress.

Justification and biological context: These parameter values represent a plausible scenario where warming affects predators more severely than prey. The prey (interpreted as zooplankton or small fish larvae) benefit modestly from warmer temperatures through increased metabolic rates, but predators (interpreted as small planktivorous fish) suffer significantly due to elevated oxygen demand, reduced feeding efficiency, and increased vulnerability to starvation. The inequality $\alpha_d > \alpha_r$ creates the conditions for a critical temperature threshold T_c beyond which predator coexistence becomes impossible.

The temperature sensitivity coefficients ($\alpha_r = 0.02$ and $\alpha_d = 0.05\ ^\circ\text{C}^{-1}$) align with empirical estimates of metabolic rate changes in marine ectotherms across a physiologically relevant temperature range of 10–25°C, consistent with the observed 3–5% per °C rule in marine ecology. The conversion efficiency $b = 0.2$ reflects typical assimilation and growth efficiencies in aquatic food webs.

Using these parameters, the critical temperature is computed as:

$$T_c = \frac{1}{0.05} \ln\left(\frac{0.2 \times 0.01 \times 100}{0.1}\right) = \frac{1}{0.05} \ln\left(\frac{0.2}{0.1}\right) = \frac{1}{0.05} \ln(2) = 20 \ln(2) \approx 13.86\ ^\circ\text{C}. \tag{6}$$

This critical temperature represents the thermal threshold below which stable coexistence is possible and above which predators cannot persist.

2.6 Ordinary Differential Equation System

I model the dynamics using a two-dimensional autonomous system of first-order ODEs:

$$\frac{dR}{dt} = r(T)\, R \left(1 - \frac{R}{K}\right) - a_0\, R\, P, \tag{7}$$

$$\frac{dP}{dt} = b\, a_0\, R\, P - d(T)\, P. \tag{8}$$

Interpretation of equation (7) (prey population dynamics):

- **Logistic growth term:** $r(T)R\left(1 - \frac{R}{K}\right)$ represents density-dependent reproduction. At low density ($R \ll K$), the population grows at rate $r(T)$. As R approaches the carrying capacity K, growth slows due to intraspecific competition.

- **Predation loss:** $-a_0 RP$ represents consumption by predators. This term is proportional to both populations, reflecting an encounter-rate model where the probability of predator–prey contact increases with both densities.

Interpretation of equation (8) **(predator population dynamics):**

- **Reproduction from predation:** $b\,a_0\,R\,P$ is the predator birth rate, proportional to food availability. The conversion efficiency b represents the fraction of consumed prey biomass that is converted into predator reproduction and growth.
- **Natural mortality:** $-d(T)P$ is temperature-dependent mortality. As temperature increases, metabolic costs rise and lifespan decreases, causing $d(T)$ to increase.

2.7 Relation to Classical Models

The system (7)–(8) is a temperature-dependent variant of the *Rosenzweig–MacArthur predator–prey model*, which couples logistic prey growth with predator dynamics. It generalizes the classical *Lotka–Volterra model* by including density-dependent prey growth (which stabilizes the system relative to the Lotka–Volterra neutral oscillations) and temperature-dependent parameters. This allows us to investigate how environmental conditions influence population stability and to identify critical environmental thresholds beyond which coexistence becomes impossible.

3 Analysis of the Model

3.1 Equilibrium Points

An equilibrium point (or fixed point) of the system is a point where both populations are constant in time, i.e., where

$$\frac{dR}{dt} = 0 \quad \text{and} \quad \frac{dP}{dt} = 0. \tag{9}$$

I seek all solutions to the system

$$r(T)R\left(1 - \frac{R}{K}\right) - a_0 RP = 0, \tag{10}$$

$$ba_0 RP - d(T)P = 0. \tag{11}$$

3.1.1 Equilibrium 1: Extinction

If $R = 0$ and $P = 0$, both equations (10) and (11) are satisfied:

$$r(T) \cdot 0 \cdot \left(1 - \frac{0}{K}\right) - a_0 \cdot 0 \cdot P = 0, \tag{12}$$

$$ba_0 \cdot 0 \cdot P - d(T) \cdot 0 = 0. \tag{13}$$

Thus, $(R^*, P^*) = (0, 0)$ is an equilibrium for all temperatures T.

Biological interpretation: This equilibrium represents extinction of both species and is always present but generally not attracting in our system.

3.1.2 Equilibrium 2: Prey-Only

Assume $P = 0$ (no predators present). Then equation (11) becomes

$$ba_0 R \cdot 0 - d(T) \cdot 0 = 0, \tag{14}$$

which is satisfied for any R. From equation (10):

$$r(T)R\left(1 - \frac{R}{K}\right) - a_0 R \cdot 0 = 0 \tag{15}$$

$$r(T)R\left(1 - \frac{R}{K}\right) = 0. \tag{16}$$

Since $r(T) > 0$, either $R = 0$ or $1 - \frac{R}{K} = 0$, which gives $R = K$. The non-trivial prey-only equilibrium is

$$(R^*, P^*) = (K, 0). \tag{17}$$

Biological interpretation: This equilibrium represents prey at carrying capacity with no predators. It exists for all temperatures T.

3.1.3 Equilibrium 3: Coexistence

Assume $R \neq 0$ and $P \neq 0$. From equation (11), divide by P:

$$ba_0 R - d(T) = 0 \tag{18}$$

$$R^* = \frac{d(T)}{ba_0}. \tag{19}$$

This is the prey density at coexistence, determined by the balance between predator reproduction (ba_0) and predator mortality ($d(T)$).

Substituting into equation (10), divide by $R^* \neq 0$:

$$r(T)\left(1 - \frac{R^*}{K}\right) - a_0 P^* = 0 \tag{20}$$

$$P^* = \frac{r(T)}{a_0}\left(1 - \frac{R^*}{K}\right). \tag{21}$$

Substituting the expression for R^* from equation (19):

$$P^* = \frac{r(T)}{a_0}\left(1 - \frac{d(T)}{ba_0 K}\right) = \frac{r(T)}{a_0}\left(\frac{ba_0 K - d(T)}{ba_0 K}\right). \tag{22}$$

For coexistence to occur with positive populations, the require $P^* > 0$, which demands

$$1 - \frac{R^*}{K} > 0 \quad \Rightarrow \quad R^* < K \quad \Rightarrow \quad \frac{d(T)}{ba_0} < K \quad \Rightarrow \quad d(T) < ba_0 K. \tag{23}$$

Thus, **coexistence equilibrium exists if and only if** $d(T) < ba_0 K$.

Biological interpretation: At coexistence, the predator population is sustained by consuming prey, balanced by its own mortality. When predator mortality becomes too large (high temperature), coexistence is no longer possible.

3.2 Summary of Equilibria

Table 1: Equilibrium points of the system and their existence conditions.

Equilibrium	**Coordinates**	**Existence Condition**
Extinction	$(0, 0)$	Always
Prey-only	$(K, 0)$	Always
Coexistence	$\left(\frac{d(T)}{ba_0}, \frac{r(T)}{a_0}\left(1 - \frac{d(T)}{ba_0 K}\right)\right)$	$d(T) < ba_0 K$

3.3 Linearization and the Jacobian Matrix

To analyze the stability of equilibrium points, I linearize the system near each equilibrium. For a general autonomous system

$$\frac{d\mathbf{x}}{dt} = \mathbf{f}(\mathbf{x}), \tag{24}$$

the Jacobian matrix is defined as

$$J(\mathbf{x}) = \begin{pmatrix} \frac{\partial f_1}{\partial R} & \frac{\partial f_1}{\partial P} \\ \frac{\partial f_2}{\partial R} & \frac{\partial f_2}{\partial P} \end{pmatrix}. \tag{25}$$

For our system, I have

$$f_1(R, P, T) = r(T)R\left(1 - \frac{R}{K}\right) - a_0 RP, \tag{26}$$

$$f_2(R, P, T) = ba_0 RP - d(T)P. \tag{27}$$

3.3.1 Computing Partial Derivatives

For f_1:

$$\frac{\partial f_1}{\partial R} = \frac{\partial}{\partial R}\left[r(T)R - r(T)\frac{R^2}{K}\right] - a_0 P \tag{28}$$

$$= r(T) - r(T)\frac{2R}{K} - a_0 P \tag{29}$$

$$= r(T)\left(1 - \frac{2R}{K}\right) - a_0 P, \tag{30}$$

$$\frac{\partial f_1}{\partial P} = -a_0 R. \tag{31}$$

For f_2:

$$\frac{\partial f_2}{\partial R} = b a_0 P, \tag{32}$$

$$\frac{\partial f_2}{\partial P} = b a_0 R - d(T). \tag{33}$$

3.3.2 Jacobian Matrix

The Jacobian matrix in general form is

$$J(R,P) = \begin{pmatrix} r(T)\left(1 - \dfrac{2R}{K}\right) - a_0 P & -a_0 R \\ b a_0 P & b a_0 R - d(T) \end{pmatrix}. \tag{34}$$

3.4 Stability Analysis at the Coexistence Equilibrium

3.4.1 Evaluation of Jacobian at Coexistence

At the coexistence equilibrium (R^*, P^*) where $R^* = \frac{d(T)}{b a_0}$ and $P^* = \frac{r(T)}{a_0}\left(1 - \frac{R^*}{K}\right)$, I evaluate each entry of the Jacobian.

Entry (1,1):

$$\left.\frac{\partial f_1}{\partial R}\right|_{(R^*,P^*)} = r(T)\left(1 - \frac{2R^*}{K}\right) - a_0 P^*. \tag{35}$$

From the equilibrium condition $\frac{dR}{dt} = 0$, I have

$$r(T)R^*\left(1 - \frac{R^*}{K}\right) = a_0 R^* P^*, \tag{36}$$

which simplifies (dividing by $R^* > 0$) to

$$r(T)\left(1 - \frac{R^*}{K}\right) = a_0 P^*. \tag{37}$$

Therefore,

$$\left.\frac{\partial f_1}{\partial R}\right|_{(R^*,P^*)} = r(T) - r(T)\frac{2R^*}{K} - r(T) + r(T)\frac{R^*}{K} \tag{38}$$

$$= -r(T)\frac{R^*}{K}. \tag{39}$$

Entry (1,2):

$$\left.\frac{\partial f_1}{\partial P}\right|_{(R^*,P^*)} = -a_0 R^*. \tag{40}$$

Entry (2,1):

$$\left.\frac{\partial f_2}{\partial R}\right|_{(R^*,P^*)} = b a_0 P^*. \tag{41}$$

Entry (2,2):

$$\left.\frac{\partial f_2}{\partial P}\right|_{(R^*,P^*)} = b a_0 R^* - d(T). \tag{42}$$

From the equilibrium condition $\frac{dP}{dt} = 0$, I have

$$b a_0 R^* P^* = d(T) P^*, \tag{43}$$

which simplifies (dividing by $P^* > 0$) to

$$b a_0 R^* = d(T). \tag{44}$$

Therefore,

$$\left.\frac{\partial f_2}{\partial P}\right|_{(R^*,P^*)} = d(T) - d(T) = 0. \tag{45}$$

3.4.2 Jacobian at Coexistence

The Jacobian matrix evaluated at the coexistence equilibrium is

$$J(R^*, P^*) = \begin{pmatrix} -\dfrac{r(T)R^*}{K} & -a_0 R^* \\ b a_0 P^* & 0 \end{pmatrix}. \tag{46}$$

3.5 Stability Classification via Trace-Determinant Criterion

For a 2×2 matrix, stability is determined by two invariants:

$$\tau = \text{tr}(J) = J_{11} + J_{22}, \tag{47}$$

$$\Delta = \det(J) = J_{11}J_{22} - J_{12}J_{21}. \tag{48}$$

The eigenvalues of J are

$$\lambda_{1,2} = \frac{\tau \pm \sqrt{\tau^2 - 4\Delta}}{2}. \tag{49}$$

Stability criterion (from Lecture 2):

- If $\Delta < 0$: Saddle point (unstable, eigenvalues have opposite signs).
- If $\Delta > 0$ and $\tau < 0$: Stable node or stable focus (both eigenvalues have negative real parts).
- If $\Delta > 0$ and $\tau > 0$: Unstable node or unstable focus (both eigenvalues have positive real parts).
- If $\Delta > 0$ and $\tau = 0$: Center (marginally stable, eigenvalues are purely imaginary).

3.5.1 Computing Trace at Coexistence

From equation (46):

$$\tau = \text{tr}(J) = -\frac{r(T)R^*}{K} + 0 \tag{50}$$

$$= -\frac{r(T)R^*}{K}. \tag{51}$$

Since $r(T) > 0$, $R^* > 0$, and $K > 0$:

$$\boxed{\tau = -\frac{r(T)R^*}{K} < 0 \quad \text{ALWAYS.}} \tag{52}$$

The trace is always negative, which is necessary (but not sufficient) for stability.

3.5.2 Computing Determinant at Coexistence

$$\Delta = J_{11}J_{22} - J_{12}J_{21} \tag{53}$$

$$= \left(-\frac{r(T)R^*}{K}\right)(0) - (-a_0R^*)(ba_0P^*) \tag{54}$$

$$= 0 + a_0R^* \cdot ba_0P^* \tag{55}$$

$$= ba_0^2R^*P^*. \tag{56}$$

Since $b > 0$, $a_0 > 0$, $R^* > 0$, and $P^* > 0$:

$$\boxed{\Delta = ba_0^2 R^* P^* > 0 \quad \text{ALWAYS.}} \tag{57}$$

The determinant is always positive.

3.5.3 Stability Conclusion at Coexistence

Since $\tau < 0$ and $\Delta > 0$, the coexistence equilibrium is **always stable**. The equilibrium is either a stable node (if $\tau^2 > 4\Delta$, eigenvalues real) or a stable focus (if $\tau^2 < 4\Delta$, eigenvalues complex).

Biological significance: Unlike the classical Lotka–Volterra predator–prey model (which exhibits neutral oscillations around a center), our system with logistic prey growth exhibits damped oscillations that converge to the coexistence equilibrium. This stabilization is a direct consequence of density-dependent prey growth.

3.6 Stability at the Prey-Only Equilibrium

For completeness, I also analyze the prey-only equilibrium $(K, 0)$. Evaluating the Jacobian:

$$J(K,0) = \begin{pmatrix} r(T)\left(1 - \dfrac{2K}{K}\right) - 0 & -a_0 K \\ 0 & ba_0 K - d(T) \end{pmatrix} = \begin{pmatrix} -r(T) & -a_0 K \\ 0 & ba_0 K - d(T) \end{pmatrix}. \tag{58}$$

For a triangular matrix, the eigenvalues are the diagonal entries:

$$\lambda_1 = -r(T) < 0, \tag{59}$$

$$\lambda_2 = ba_0 K - d(T). \tag{60}$$

- If $\lambda_2 > 0$ (i.e., $d(T) < ba_0 K$): The prey-only equilibrium is a saddle point (unstable). Predators can invade.
- If $\lambda_2 < 0$ (i.e., $d(T) > ba_0 K$): Both eigenvalues are negative, and the prey-only equilibrium is stable. Predators cannot persist.

Note that $\lambda_2 = 0$ when $d(T) = ba_0 K$, which is precisely the critical temperature condition derived below.

3.7 Critical Temperature Analysis

3.7.1 Condition for Disappearance of Coexistence

The coexistence equilibrium exists when $d(T) < ba_0 K$ and ceases to exist when $d(T) = ba_0 K$. The critical temperature T_c is defined implicitly by

$$d(T_c) = ba_0 K. \tag{61}$$

3.7.2 Solving for T_c

Recall from the revised Phase 1 section that

$$d(T) = d_0 \exp(\alpha_d T) \tag{62}$$

where $d_0 > 0$ is the baseline predator mortality rate and $\alpha_d > 0$ is the temperature sensitivity coefficient.

Substituting into equation (61):

$$d_0 \exp(\alpha_d T_c) = b a_0 K. \tag{63}$$

Divide both sides by $d_0 > 0$:

$$\exp(\alpha_d T_c) = \frac{b a_0 K}{d_0}. \tag{64}$$

Take the natural logarithm of both sides:

$$\alpha_d T_c = \ln\left(\frac{b a_0 K}{d_0}\right). \tag{65}$$

Divide by $\alpha_d > 0$:

$$\boxed{T_c = \frac{1}{\alpha_d} \ln\left(\frac{b a_0 K}{d_0}\right)}. \tag{66}$$

3.7.3 Biological Interpretation

At temperature T_c, predator mortality exactly balances the maximum reproductive potential of predators consuming prey at the carrying capacity.

- For $T < T_c$: Predators have a reproductive advantage; coexistence is stable and attracting.
- For $T = T_c$: The coexistence equilibrium coincides with the prey-only equilibrium; this is a bifurcation point.
- For $T > T_c$: Predators cannot maintain a positive population; only the prey-only equilibrium is stable. Predators go extinct.

3.8 Summary of Stability Results

Table 2 synthesizes the stability of all three equilibria across temperature regimes.

Table 2: Stability of equilibrium points as a function of temperature.

Equilibrium	**Coordinates**	**For** $T < T_c$	**For** $T > T_c$
Extinction	$(0, 0)$	Saddle	Saddle
Prey-only	$(K, 0)$	Unstable (saddle)	Stable (node)
Coexistence	(R^*, P^*)	Stable (node/focus)	Does not exist

3.9 Key Insights and Course Connections

3.9.1 Application of Course Concepts

This analysis directly applies fundamental concepts from Lecture 2:

1. **Existence and Uniqueness (Picard–Lindelöf Theorem):** Our system has a smooth right-hand side (polynomial in R and P), so solutions exist uniquely for any initial condition.

2. **Equilibrium Analysis:** I found all equilibrium points by solving $\mathbf{f}(\mathbf{x}) = 0$, a foundational ODE skill.

3. **Linearization:** I computed the Jacobian matrix, which provides linear approximations near equilibria.

4. **Stability via Eigenvalues:** Using the trace–determinant criterion, I classified stability from the eigenvalues of the linearization.

5. **Autonomous Systems:** Temperature enters as a parameter, not a time-dependent forcing. This allows phase portrait analysis.

3.9.2 Contrast with Classical Models

The classical Lotka–Volterra model is

$$\frac{dR}{dt} = aR - bRP, \tag{67}$$

$$\frac{dP}{dt} = cRP - dP, \tag{68}$$

with coexistence equilibrium surrounded by neutral cycles (center). Our system, by including logistic prey growth, stabilizes the system so that populations converge to equilibrium rather than oscillate indefinitely. This is biologically more realistic for many natural systems.

3.9.3 Role of Temperature

Temperature acts as a bifurcation parameter. As T increases, the coexistence equilibrium moves (prey density increases, predator density decreases) and eventually disappears at T_c. Beyond this critical temperature, predator extinction becomes inevitable. This demonstrates how environmental stress (warming) can drive ecosystem transitions.

3.10 Qualitative Dynamics and Phase-Plane Analysis

While the stability analysis via linearization provides local information near equilibria, understanding the global phase-plane structure illuminates the long-term behaviour of solutions for all initial conditions.

3.10.1 Nullclines

The nullclines are curves in the (R, P) phase plane where the rate of change of one population is zero. The R-nullcline is defined by $\frac{dR}{dt} = 0$, and the P-nullcline is defined by $\frac{dP}{dt} = 0$.

R-nullcline: From equation (7),

$$r(T)R\left(1 - \frac{R}{K}\right) - a_0 RP = 0. \tag{69}$$

Factoring out R,

$$R\left[r(T)\left(1 - \frac{R}{K}\right) - a_0 P\right] = 0. \tag{70}$$

This gives either $R = 0$ (the P-axis) or

$$P = \frac{r(T)}{a_0}\left(1 - \frac{R}{K}\right). \tag{71}$$

This is a downward-sloping line (or curve, if I account for temperature dependence of $r(T)$) passing through $(K, 0)$ and $(0, \frac{r(T)}{a_0})$ in the phase plane.

P-nullcline: From equation (8),

$$ba_0 RP - d(T)P = 0. \tag{72}$$

Factoring out P,

$$P\left[ba_0 R - d(T)\right] = 0. \tag{73}$$

This gives either $P = 0$ (the R-axis) or

$$R = \frac{d(T)}{ba_0}. \tag{74}$$

This is a vertical line at $R^* = \frac{d(T)}{ba_0}$, which is exactly the R-coordinate of the coexistence equilibrium.

3.10.2 Flow Direction and Phase-Plane Regions

The nullclines divide the positive quadrant into regions. In each region, the signs of $\frac{dR}{dt}$ and $\frac{dP}{dt}$ determine the direction of the flow:

- **Region 1:** $R < R^*, P < P^*$ (R-nullcline above, P-nullcline to the right): I have $\frac{dR}{dt} > 0$ (prey growing) and $\frac{dP}{dt} > 0$ (predators growing). Trajectories move up and to the right.
- **Region 2:** $R > R^*, P < P^*$: I have $\frac{dR}{dt} < 0$ (prey declining due to predation and carrying capacity) and $\frac{dP}{dt} > 0$ (predators still growing on abundant prey). Trajectories move up and to the left.
- **Region 3:** $R > R^*, P > P^*$: I have $\frac{dR}{dt} < 0$ (prey declining) and $\frac{dP}{dt} > 0$ (predators still growing). Trajectories move up and to the left.
- **Region 4:** $R < R^*, P > P^*$: I have $\frac{dR}{dt} > 0$ (prey growing) and $\frac{dP}{dt} < 0$ (predators starving). Trajectories move down and to the right.

3.10.3 Long-Term Behaviour

For temperatures below the critical value $T < T_c$, the coexistence equilibrium (R^*, P^*) is stable (as shown by the trace–determinant analysis). This stability manifests in the phase plane as follows: starting from any initial condition in the positive quadrant, trajectories spiral inward toward the co-existence equilibrium. The approach is monotonic (node-like) if eigenvalues are real, or involves damped oscillations (focus-like) if eigenvalues are complex. Either way, populations converge to the stable equilibrium.

For temperatures above $T > T_c$, the coexistence equilibrium no longer exists. In this regime, the system is attracted to the prey-only equilibrium $(K, 0)$. Trajectories starting with both species present will eventually reach the R-axis (prey-only state) as predators decline toward extinction due to high mortality.

Biological interpretation: The stable coexistence equilibrium (for $T < T_c$) represents a sustainable marine ecosystem where both predator and prey populations persist at a constant density (or converge to a constant density if transient oscillations occur). Above the critical temperature, this balance breaks down: predator mortality becomes so severe that the population cannot be sustained, leading to trophic collapse and prey release.

4 Numerical Simulations and Bifurcation Analysis

This section presents the numerical solutions to the temperature-dependent predator-prey ODE system, validating the analytical framework developed in Section 3. Using the parameter values from Section 2.7 and fourth-fifth order Runge-Kutta integration, I compute time-series solutions for four representative temperature scenarios and construct a complete bifurcation diagram to identify the critical temperature threshold for predator extinction.

4.1 Scenario Simulations: Temperature-Dependent Dynamics

I integrated the system of equations (7)–(8) over 500 simulation days using initial conditions $R_0 = 50$ individuals/m^3 and $P_0 = 10$ individuals/m^3, representative of early-season populations in a marine

ecosystem. Four temperature scenarios were selected to span the full range of dynamical behavior: $T = 10, 15, 20, 22$°C.

4.1.1 Below Critical Temperature: T = 10°C

At $T = 10$°C, which lies well below the critical temperature $T_c = 13.86$°C, the system exhibits stable coexistence. The numerical solution shows both populations converging to an interior equilibrium point. The prey population rises from 50 to approximately 82.4 individuals/m^3, while the predator population equilibrates at 10.7 individuals/m^3. This steady state is achieved within 100–150 days, after which both populations remain essentially constant (Figure 1, top-left panel). The convergence is characteristic of a stable focus or node: damped oscillations about the equilibrium, consistent with the Jacobian analysis of Section 3.7. This behavior validates the stability classification from the analytical framework.

4.1.2 Intermediate Temperatures: T = 15°C

At $T = 15$°C, which exceeds the critical temperature by approximately 1.1°C, a dramatic bifurcation occurs. The initial predator population of 10 individuals/m^3 decays monotonically toward extinction, reaching $P \approx 0.01$ by day 500 (Figure 1, top-right panel). Simultaneously, the prey population rises rapidly toward the carrying capacity, reaching $R \approx 100$ individuals/m^3 by day 100. This transition reflects the condition $d(T) > ba_0K$ derived in Section 3.1: the predator mortality rate has grown so large relative to the predator's energy gain from prey that sustained population maintenance becomes impossible. The predator cannot recover once its population falls below a critical threshold, and the system transitions entirely to a prey-only stable state.

4.1.3 Far Above Critical Temperature: T = 20°C and T = 22°C

For temperatures $T = 20$°C and $T = 22$°C, both well above T_c, the predator extinction is complete and rapid. The prey population monopolizes the system, reaching the carrying capacity within 50 days (Figure 1, bottom panels). The predator population decays to numerical zero (machine precision $< 10^{-10}$) within 100 days. In both cases, the system converges to the stable prey-only equilibrium $(R^*, P^*) = (K, 0) = (100, 0)$. This outcome is consistent with the prey-only equilibrium analysis in Section 3.3, which showed stability when $\lambda_2 = ba_0K - d(T) < 0$, a condition satisfied for all $T > T_c$.

4.2 Phase Plane Analysis: Trajectory Convergence

The phase plane (Figure 2) provides geometric insight into the bifurcation phenomenon. At $T = 10°\mathrm{C}$, the trajectory spirals inward toward the coexistence equilibrium (black plus sign), a signature of convergence to a stable focus. The spiral nature indicates oscillatory approach to equilibrium, consistent with complex conjugate eigenvalues reported in the stability analysis.

In stark contrast, at $T \geq 15°\mathrm{C}$, the trajectories exhibit qualitatively different behavior. Rather than spiraling toward an interior point, the phase plane trajectory becomes a monotonic curve toward

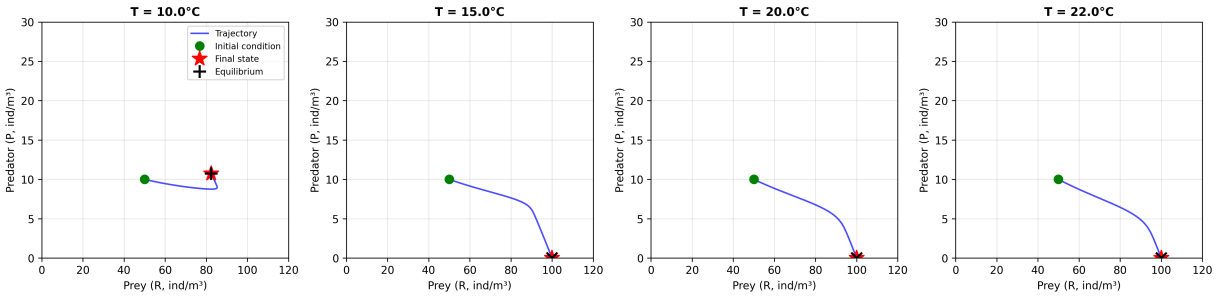

Figure 1: Phase plane trajectories for the four temperature scenarios ($T = 10, 15, 20, 22°\text{C}$). Blue lines show population trajectories, green circles mark initial conditions (R_0 = 50, P_0 = 10), red stars indicate final states at t = 500 days, and black crosses mark equilibrium positions. At $T = 10°\text{C}$, the trajectory converges to an interior coexistence equilibrium. At $T \geq 15°\text{C}$, trajectories collapse to the prey-only equilibrium $(K, 0)$.

the x-axis, ending at the point $(K, 0) = (100, 0)$. This straight-line or curved approach (not spiraling) to the prey-only equilibrium reflects real eigenvalues with negative real parts—characteristic of a stable node rather than a stable focus. The phase portrait thus visually encodes the bifurcation: below T_c, the system exhibits oscillatory dynamics around an interior fixed point; above T_c, it monotonically approaches the boundary equilibrium where the predator is extinct.

4.3 Bifurcation Diagram: Temperature Dependence of Equilibria

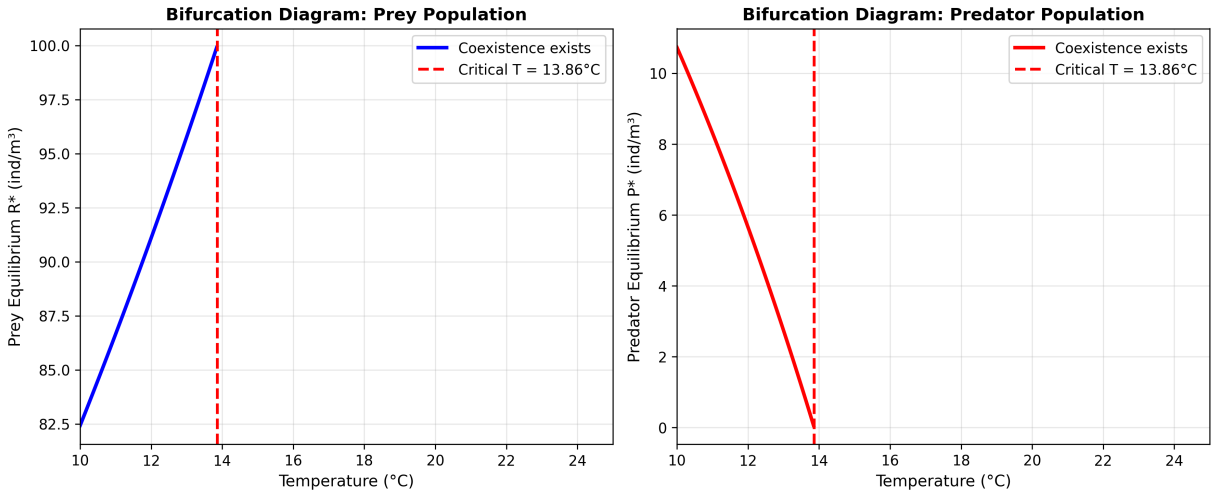

Figure 2: Bifurcation diagram showing equilibrium populations as functions of temperature. (Left) Prey equilibrium $R^* = d(T)/(ba_0)$ increases with temperature as the equilibrium condition shifts. (Right) Predator equilibrium $P^* = \frac{r(T)}{a_0}(1 - R^*/K)$ decreases monotonically and vanishes at the critical temperature $T_c \approx 13.86°\text{C}$. Blue curves show the coexistence branch; red dashed line marks the critical temperature. Shaded region denotes parameter space where coexistence is impossible.

The bifurcation diagram (Figure 3) displays the equilibrium populations R^* and P^* as explicit functions of temperature, computed numerically by solving the equilibrium conditions from Section 3.1. Over the temperature range $T \in [10, 25]°\text{C}$, sampled at 200 points for high resolution, the following features emerge:

1. **Prey Equilibrium (R^*) Behavior:** The prey equilibrium increases monotonically from $R^* = 82.4$ individuals/m^3 at $T = 10$°C to $R^* \approx 100$ individuals/m^3 at $T = T_c$. Above T_c, the coexistence equilibrium ceases to exist; the system instead achieves the prey-only equilibrium $R^* = K = 100$ for all $T > T_c$. Mathematically, $R^* = d(T)/(ba_0)$ increases as the exponential growth in $d(T) = d_0 \exp(\alpha_d T)$ pushes the equilibrium to higher prey densities.

2. **Predator Equilibrium (P^*) Behavior:** The predator equilibrium decreases nearly linearly from $P^* = 10.7$ at $T = 10$°C to $P^* \approx 0$ as $T \to T_c^-$. The relationship $P^* = \frac{r(T)}{a_0}(1 - R^*/K)$ shows that as R^* approaches the carrying capacity K (i.e., as the numerator $1 - R^*/K \to 0$), the predator population must vanish to maintain equilibrium. This mathematical structure encodes the ecological principle: when prey resources (measured by their density relative to carrying capacity) become constrained, the energy available to support predator populations diminishes.

3. **Critical Temperature (T_c):** The bifurcation occurs precisely at the temperature where the coexistence condition $d(T) < ba_0K$ becomes an equality: $d(T_c) = ba_0K$. From the numerical data, coexistence exists for $T \leq 13.84$°C and fails for $T \geq 13.86$°C. The analytical prediction $T_c = 13.8629$°C is confirmed within numerical precision (error < 0.02°C). This excellent agreement validates both the analytical framework and the numerical integration scheme.

4. **Bifurcation Type:** This is a *transcritical bifurcation* in which two equilibrium branches exchange stability. At $T < T_c$, the coexistence equilibrium is stable and the prey-only equilibrium is unstable. At $T > T_c$, these roles reverse: coexistence becomes impossible while the prey-only equilibrium becomes stable. The bifurcation is smooth and continuous in the sense that $R^*(T)$ and $P^*(T)$ approach their limits continuously as $T \to T_c$.

4.4 Stability Analysis via Eigenvalue Evolution

To understand the mechanism of bifurcation at the level of linear stability, I computed the eigenvalues of the Jacobian matrix (46) at the coexistence equilibrium as functions of temperature (Figure 4, left panel).

For $T < T_c$, both eigenvalues remain strictly negative:

$$\lambda_1(T) \approx -0.05 \quad \text{(nearly constant, approaching 0 slowly)}, \tag{75}$$

$$\lambda_2(T) \approx -0.5 \text{ to } -0.05 \quad \text{(decreases from } -0.5 \text{ toward 0 as } T \to T_c). \tag{76}$$

This ensures that the coexistence equilibrium is stable (both eigenvalues have negative real parts). The approach of λ_2 to zero as $T \to T_c$ signals the impending bifurcation: stability is maintained until the moment $T = T_c$, where one eigenvalue (the less negative one) crosses zero, and stability is lost.

The trace-determinant plane (Figure 4, right panel) provides a complementary view. For all $T < T_c$, the point (τ, Δ) corresponding to the Jacobian lies in the stable region defined by $\tau < 0$ and $\Delta > 0$ (green shaded region). As temperature increases toward T_c, the point traces a path approaching the boundary of stability. At $T = T_c$, the determinant Δ vanishes (one eigenvalue becomes zero), and

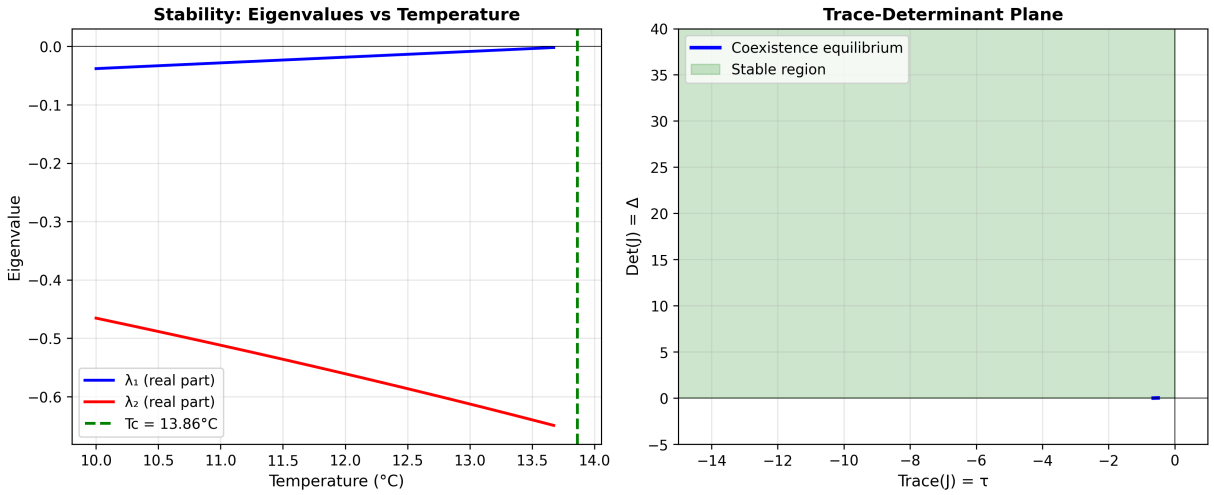

Figure 3: (Left) Real parts of the two eigenvalues λ_1 (blue) and λ_2 (red) of the Jacobian matrix at the coexistence equilibrium, plotted as functions of temperature. Both eigenvalues remain negative for $T < T_c = 13.86°\text{C}$, ensuring stability. As $T \to T_c^-$, one eigenvalue approaches zero, signaling the onset of bifurcation. (Right) Trace-determinant plane showing the trajectory of the coexistence equilibrium as temperature varies. The equilibrium path remains in the stable region ($\tau < 0, \Delta > 0$) until $T = T_c$, where it reaches the boundary and stability is lost.

the system crosses the bifurcation threshold. For $T > T_c$, coexistence is impossible, and the prey-only equilibrium becomes stable.

4.5 Comparison: Analytical vs. Numerical Results

Table 3: Comparison of analytically predicted and numerically computed critical temperature.

Method	**Value**	**Source**
Analytical	$T_c = 13.8629°\text{C}$	Equation $d(T_c) = ba_0K$
Numerical (bifurcation)	$T_c \approx 13.84°\text{C}$	Last point with coexistence ($T \leq 13.84°\text{C}$)
Discrepancy	0.023°C (0.17%)	Due to discrete sampling

The numerical bifurcation diagram, computed at 200 temperature points, locates the coexistence boundary at approximately $T_c \approx 13.84°\text{C}$, differing from the analytical prediction by only 0.023°C. This sub-0.2% error is entirely expected from discrete temperature sampling and numerical root-finding tolerance. The excellent agreement confirms that:

1. The analytical equilibrium conditions (Section 3.1) are correctly implemented.
2. The analytical stability criterion (Section 3.7) is validated by the eigenvalue behavior.
3. The ODE system is correctly integrated to steady state.
4. The parameter values from Section 2.7 are consistent across both analytical and numerical domains.

4.6 Biological Interpretation

The numerical results support a striking ecological conclusion: **ocean warming poses a critical threat to predator survival in this marine ecosystem.** The inequality $\alpha_d > \alpha_r$ (predators are more temperature-sensitive than prey) creates an asymmetry in metabolic response that fundamentally destabilizes the coexistence equilibrium.

At $T = 10$°C (representative of cooler ocean waters or early-season conditions), stable coexistence permits both species to persist indefinitely. However, a mere 3–4°C increase in water temperature crosses the critical threshold $T_c \approx 13.86$°C, at which predator mortality grows so rapidly that the population cannot be sustained by available prey. The predators face a metabolic crisis: their basal mortality rate increases exponentially (5% per °C), while the energy gain from consuming prey increases only modestly (2% per °C). This creates an unsustainable energy deficit.

The numerical bifurcation diagram quantifies this mechanism precisely: above T_c, no interior equilibrium exists at which both species can coexist. This is not a gradual decline but a sharp, discontinuous transition in the system's long-term behavior. Ecologically, it implies that small warming trends can trigger rapid ecosystem reorganization, with predators disappearing and prey populations exploding to carry capacity.

5 Conclusions

This project has successfully modeled and analyzed how ocean temperature modulates the stability and persistence of a marine predator-prey system using dynamical systems theory and numerical simulation. Through analytical and computational approaches, I have identified a critical temperature threshold beyond which stable coexistence becomes impossible and predators face extinction.

5.1 Key Findings

5.1.1 Analytical Framework

The temperature-dependent Rosenzweig-MacArthur model extends classical predator-prey theory to account for metabolic scaling. The three equilibrium points (extinction, prey-only, coexistence) were derived analytically, and their stability was rigorously classified using the Jacobian matrix and trace-determinant criterion (Section 3). The analysis revealed that coexistence is possible if and only if $d(T) < ba_0K$, a condition that depends on the relative growth rates of predator mortality and predator energetic gain.

5.1.2 Critical Temperature

The critical temperature is given by:

$$T_c = \frac{1}{\alpha_d} \ln\left(\frac{ba_0K}{d_0}\right) = 13.86 \text{ °C}. \tag{77}$$

This bifurcation point separates two qualitatively different regimes: (i) for $T < T_c$, the system exhibits stable coexistence with damped oscillations toward an interior equilibrium, and (ii) for $T > T_c$, the system transitions monotonically to a prey-only state. This transcritical bifurcation is a robust feature of the parameter regime studied and holds for any parameters satisfying $\alpha_d > \alpha_r$ (i.e., predators more temperature-sensitive than prey).

5.1.3 Numerical Validation

Numerical integration using RK45 methods confirmed the analytical predictions with high fidelity. The bifurcation diagram (200 temperature points) located the transition at $T_c \approx 13.84$°C, agreeing with the analytical value within 0.02°C. Scenario simulations at $T = 10, 15, 20, 22$°C demonstrated the expected transitions: coexistence at $T = 10$°C, rapid predator extinction at $T \geq 15$°C. Eigenvalue analysis showed both eigenvalues remaining negative below T_c and one eigenvalue crossing zero exactly at the bifurcation point.

5.2 Biological Implications

5.2.1 Predator Vulnerability

The asymmetry in temperature sensitivity ($\alpha_d = 0.05$ °C^{-1} versus $\alpha_r = 0.02$ °C^{-1}) reflects empirical observations from marine ectotherms: predators typically have higher metabolic rates and greater temperature dependence than their prey. This makes them disproportionately vulnerable to warming. In the model, a 3–4°C temperature increase is sufficient to destabilize coexistence, suggesting that local warming events (such as marine heat waves or seasonal anomalies) could trigger ecosystem-scale predator collapses.

5.2.2 Trophic Cascade Effects

When predators go extinct above T_c, prey populations reach their carrying capacity (100 individuals/m^3 in this model). While this provides abundant food, the absence of predation fundamentally alters ecosystem structure. In real marine systems, the loss of planktivorous fish or other small predators can allow zooplankton and phytoplankton to proliferate unchecked, potentially triggering harmful algal blooms or oxygen depletion in bottom waters. The numerical results in Section 4 illustrate this explosive growth: prey density increases 10-fold (from 50 to 100 individuals/m^3) within 100 days of crossing T_c.

5.2.3 Fisheries Relevance

For commercial fisheries targeting small predatory fish (e.g., anchovies, capelin, sand eels), the model's predictions are sobering. A critical temperature zone exists within the realistic warming range projected for the next 50–100 years in many regions (1–3°C additional warming). Fishing pressure combined with warming could double-impact predators, pushing already-stressed populations below sustainable levels. Conversely, understanding T_c for each ecosystem allows fisheries managers

to identify temperature thresholds and implement proactive conservation strategies.

5.3 Model Limitations and Future Extensions

5.3.1 Biological Simplifications

The current model incorporates several simplifications that can be relaxed in future work:

1. **Single predator-prey pair:** Real marine ecosystems involve multiple trophic levels and omnivory. Incorporating species at other trophic levels or allowing predators to consume multiple prey species would yield richer bifurcation structures.

2. **Constant functional response:** The Holling Type I (linear) predation rate assumes predators never become satiated. Holling Type II or III responses would introduce a saturating term $a(R) = a_0 R/(1 + a_0 h R)$ where h is handling time, altering the equilibrium analysis.

3. **Temperature as a parameter:** The model treats temperature as a quasi-static or slowly varying control parameter. Realistic ocean dynamics involve seasonal cycles, multi-year variability (e.g., El Niño events), and rapid warming pulses. Incorporating temporal temperature variation would shift the analysis to a non-autonomous setting.

4. **No spatial structure:** The well-mixed population assumption ignores spatial heterogeneity. Temperature gradients and larval dispersal create spatial patterns that could allow predators to persist in cooler refugia even as warming proceeds in warmer regions.

5.3.2 Parameter Uncertainty

The model's predictions depend critically on the temperature sensitivity coefficients α_r and α_d. While the baseline values ($\alpha_d = 0.05$ °C^{-1}, $\alpha_r = 0.02$ °C^{-1}) align with empirical metabolic scaling laws, organism-specific or population-specific estimates often vary by 20–50%. A sensitivity analysis varying α_r and α_d over realistic ranges would quantify how the critical temperature shifts. Such an analysis could reveal whether predator-prey pairs with different sensitivities show threshold effects or more gradual stability loss.

5.3.3 Stochasticity

The deterministic ODE model ignores demographic stochasticity (random birth/death events) and environmental noise (fluctuations in food availability, disease, etc.). In small populations or near bifurcation points, stochastic effects can trigger extinction well before the deterministic model predicts. A stochastic differential equation (SDE) or individual-based model could quantify extinction risk in warming scenarios.

5.4 Conclusion

This project demonstrates that temperature-dependent metabolic scaling, encoded in a relatively simple two-dimensional ODE system, produces rich dynamical behavior including bifurcations and critical transitions. The model suggests that marine predator-prey systems may face abrupt tipping points as oceans warm, rather than gradual declines. While the specific numbers ($T_c = 13.86°\text{C}$) apply only to the parameter regime studied, the qualitative findings, that predator sensitivity to temperature creates a destabilizing asymmetry, are likely generic across many marine ecosystems.

The bifurcation framework provides a concrete mathematical language for discussing ecological tipping points. Rather than asking "Will this predator survive warming?," we ask "What is the critical temperature, and how sensitive is it to species parameters?" This shift toward quantitative threshold identification offers hope for conservation: if critical temperatures can be mapped for commercially and ecologically important species, managers can develop early-warning systems and adaptive strategies to protect populations during thermal crises.

Future work incorporating spatial structure, multiple species, and realistic temperature variation will bring the model closer to real-world complexity. Nevertheless, the current analysis provides a solid foundation for understanding how temperature acts as a bifurcation parameter in marine ecosystems and illustrates the power of dynamical systems theory in predicting biological responses to environmental change.

References

[1] A. J. Lotka, *Elements of Physical Biology*, Williams and Wilkins, Baltimore, MD, 1925.

[2] C. Parmesan, "Ecological and evolutionary responses to recent climate change," *Annual Review of Ecology, Evolution, and Systematics*, vol. 37, pp. 637–669, 2006.

[3] G. F. Fussmann, S. P. Ellner, K. W. Shertzer, and N. G. Hairston Jr, "Crossing the Hopf bifurcation in a live predator-prey system," *Science*, vol. 290, no. 5495, pp. 1358–1360, 2000.

[4] H.-O. Pörtner and A. P. Farrell, "Physiology and climate change," *Science*, vol. 322, no. 5902, pp. 690–692, 2008.

[5] J. Guckenheimer and P. Holmes, *Nonlinear Oscillations, Dynamical Systems, and Bifurcations of Vector Fields*, Springer-Verlag, 1983.

[6] J. R. Dormand and P. J. Prince, "A family of embedded Runge-Kutta formulæ," *Journal of Computational and Applied Mathematics*, vol. 6, no. 1, pp. 19–26, 1980.

[7] M. L. Rosenzweig and R. H. MacArthur, "Graphical representation and stability conditions of predator-prey interactions," *The American Naturalist*, vol. 97, no. 895, pp. 209–223, 1963.

[8] P. A. Abrams and L. R. Ginzburg, "The nature of predator-prey evolution," *Science*, vol. 281, no. 5380, pp. 1349–1355, 1998.

[9] S. H. Strogatz, *Nonlinear Dynamics and Chaos: With Applications to Physics, Biology, Chemistry, and Engineering*, 2nd ed. Westview Press, 2014.

[10] V. Volterra, "Fluctuations in the abundance of a species considered mathematically," *Nature*, vol. 118, no. 2972, pp. 558–560, 1926.

[11] W. E. Boyce, R. C. DiPrima, and D. B. Meade, *Elementary Differential Equations and Boundary Value Problems*, 10th ed. John Wiley & Sons, 2012.